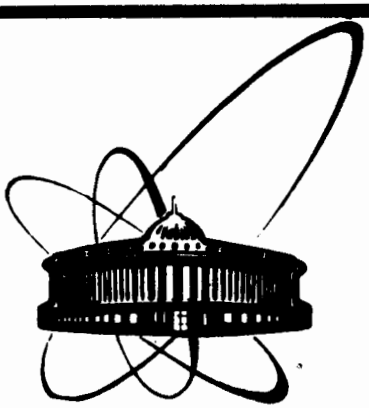

объединенный
институт
ядерных
исследований
дубна

E12-89-162

V.V.Ovchinnikov, V.D.Seleznev*, V.V.Surguchev*,
V.I.Kuznetsov

CONTROLLABLE CHANGES IN THE POROUS STRUCTURE OF POLYMERIC NUCLEAR MEMBRANES

Submitted to "Journal of Membrane Science"

* Department of Molecular Physics,
Urals Polytechnical Institute, Sverdlovsk, USSR

1989

1. Introduction

Membrane separation of liquid and gaseous media is largely based on polymeric materials. Great success has been achieved in creating polymeric membranes of different structure and properties, manufactured both by traditional methods (wet and dry forming) and by physical or chemical modification of polymers. For instance, the amorphous-crystalline polyethylene terephthalate (PETP) film is successfully modified by crystalline or noncrystalline solvents[1]. So, the treatment of PETP by the water-acetone solvent leads to a considerable increase in the crystallinity rate of the polymer, which in its turn leads to a greater number of defects of the polymeric matrix. This considerably affects permeability of the samples [2].

An interesting approach to polymeric modification is proposed in papers [3-5], where deformation of the polymeric films in the adsorption-active medium is investigated. It was found that deformation of glassy and crystalline polymer in H-propanole is accompanied with formation of highly dispersed porous structure (microcracks were about 10 nm in size). In the last decade polymeric membranes of a new type appeared in the USSR. They are nuclear microfilters with the uniform structure and almost cylinder-shaped pores [6]. These filtration materials are suitable for the use as the modelling porous media owing to a possibility of checking the geometry of identical pores during any processes. For example, in paper [7] the change in the effective pore size is used to investigate the thermo-modification of the nuclear PETP membranes tending to both decrease and increase in permeability. In paper [8] a possibility of increasing the pore size by applying the external load was shown for the same membranes. It turned out that the concentration of stresses appears in the around-pore areas of the membrane under load. Under certain conditions this leads to large deformation of around-pore zones of the polymeric matrix and to the increase in permeability.

2. Apparatus and procedure

The deformation of the porous structure of the PETP nuclear membranes loaded by the excessive gas pressure was investigated by the gas dynamics method [9] at the experimental apparatus shown schematically in Fig. 1. The working chamber 11 is assembled of two volumes fixed on the common flange with the filter holder 13 with

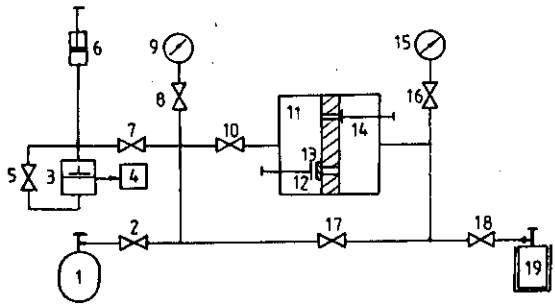

Fig.1.Schematic view of the experimental apparatus.1 - gas cylinder; 2,7,10,17,18 - valves; 3 - capacitive micromanometer; 4 - frequency-meter; 5 - by-pass valve; 6 - graduated cylinder with piston; 8 - manometer; 11 - working chamber; 12 - nuclear membrane plug; 13,14 - by-pass plug; 15 - vacuum gage; 19 - adsorption pump.

the membrane. The membrane samples were loaded according to the scheme of the biaxial tension of a film at room temperature /8/. The dynamic vacuum on one side of the membrane was maintained by the adsorption pump, but on the other side a gas (argon or xenon) was fed in through the controlling valve to obtain the loading pressure P_l. In most cases the feed rate was about 0.13 MPa/min. It was achieved when the plug 14 was opened. In some experiments there was a "shock" loading, i.e. a gas was fed in with the plugs 12 and 14 closed, the plug 12 of the membrane being then opened at the zero time. The PETP nuclear membrane samples endured from 2 to 20 min in the loaded state under the pressure P_l. The pressure P_l was stabilized with the help of the controlling valve 2.

The off-loading of the samples was carried out by opening the by-pass valve. The rate of the pressure equalization in the working chamber was about 0.2-0.3 MPa/min.

After the loading and off-loading cycle ended, the gas flow rate (at a small pressure difference) and its dependence on the time from the beginning of the off-loading were measured in order to reveal the relaxation processes characteristic of polymeric films. The pore size was checked by the steady gas flow method on the apparatus shown in Fig. 1 /8/ after the visible relaxation processes ended. The gas flow rate was determined with the help of the piston-type flowmeter 6 and the capacitive micromanometer 3 connected with

the frequency-meter 4 /10/, the by-pass valve 5 being closed. The gas pressure drop before the membrane was compensated for by the motion of the piston of the graduated cylinder 6 with keeping watch on the micromanometer generator frequency. The volume gas flow rate was found by the equation

$$Q = \frac{\pi D^2}{4} \cdot \frac{\Delta l}{\Delta t}, \qquad (1)$$

where Δl is the displacement of the piston of the piston-type flowmeter for the time Δt; D is the diameter of the piston. To find the effective pore size, it is convenient to use the flow rate Q^* in the form

$$Q^* = \frac{Q P_o}{\Delta P}, \qquad (2)$$

where P_o is the gas pressure at the membrane inlet; ΔP is the pressure difference. The gas dynamics technique of measuring the effective pore radius consisted in plotting the calibration curve $W = f(\lg \delta)$ for a nuclear membrane with the known pore geometry. (Here W is the non-dimensional flow rate; δ is the rarefaction parameter which includes the pore radius). Then one plots the function $W = f(\lg \delta)$ for a membrane with the unknown pore geometry and, as the dependence of the non-dimensional gas flow rate is a universal curve /9/, one makes it coincident with the calibration function by selecting R and finds the sought-for pore size. The error does not exceed 5%, for pores over 20 nm.

3. Experimental results

The dependence $R/R_o = f(P_l)$ in Fig. 2 (R is the gas-dynamic pore radius after the loading and off-loading cycle for the loading pressure P_l; R_o is the initial gas-dynamic pore radius of the unloaded membrane) was determihed for the samples with the pore density about 10^7 cm^{-2} and the working surface (0.95 ± 0.03) cm^2. The behavior of the curves shows that there is no pore growth effect when P_l is less than some limit value of 0.08-0.12 MPa. In this case the deformations in the around-pore areas of the membrane are elastic and the growth of the pores is not irreversible. When the loading pressure exceeds the threshold value, the growth of the pores is observed, it being the function of the initial radius R_o. As mentioned in paper /8/, the pores of the loaded membranes are noticeably growing in size because stresses close to the yield stress of the polymer appear in the around-pore zones. These stresses cause a plastic flow of the membrane material around the pores leading to

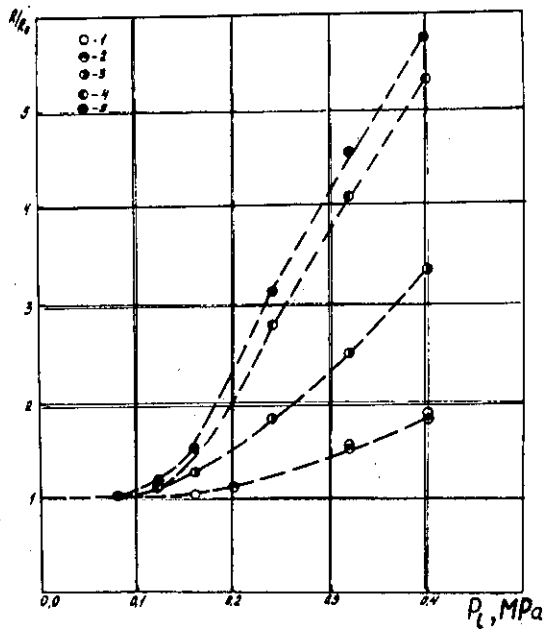

Fig. 2. Experimental relation $R/R_o=f(P_l)$ for the samples with $n=10^7$ cm^{-2} and $S=0.95$ cm^2. 1,2,3,4,5, R_o=57; 75; 18.9; 10.8; 10.2 nm.

their growth. The dependence of the increase in the membrane permeability on the initial pore radii is illustrated in Fig. 3. The samples with the pore density about $(3\div4)\cdot10^8$ cm^{-2} has equal surfaces. The curves show that within the same pressure load the value of R/R_o sharply increases as the membrane pore radii decrease (less than 10 nm). This figure also shows the dependence obtained for the samples with the pore density about $1\cdot10^7$ cm^{-2}. The comparison of the curves allows the conclusion that the effect of the pore growth is a function not only of P_l and R_o, but also of n, i.e. when the initial porosity of a sample decreases (with other conditions being equal) a considerable pore growth is observed starting from a larger value of R_o. The dependence of the pore growth effect in the membranes under load on the working surface of the samples was also found. Figures 4 and 5 show the experimental functions $R/R_o=f(P_l)$ and $R/R_o=f(R_o)$ obtained by loading the membranes with working surface $S=0.196$ cm^2 and the pore density of $(3\div4)10^8$ cm^{-2}. It follows from curves in Fig. 4 the pore expansion effects, corresponding to the dependences in Fig. 2, appear in the samples with a smaller working

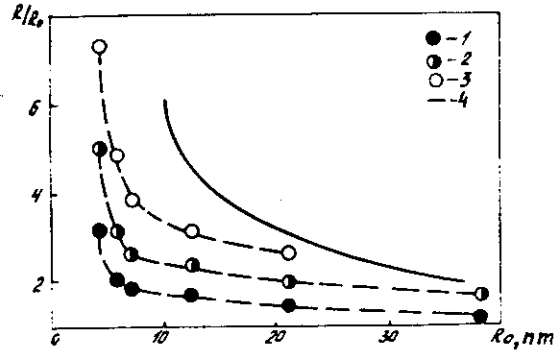

Fig. 3. Experimental relation $R/R_o=f(R_o)$ for the samples with $n=(3\div4)\cdot10^8$ cm^{-2} and $S=0.95$ cm^2. 1,2,3, $P_l=0.24$; 0.32; 0.4 MPa; 4, $P_l=0.4$ MPa, $n\simeq10^7$ cm^{-2}.

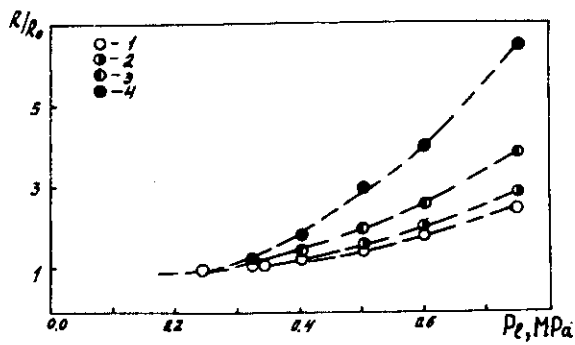

Fig. 4. Experimental relation $R/R_o=f(P_l)$ for the samples with $n=(3\div4)10^8$ cm^{-2} and $S=0.196$ cm^2. 1,2,3,4, $R_o=5$; 7; 10.5; 20.6 nm.

surface at a greater pressure load. Thus, in this part of the paper we have experimentally found the relation between the pore growth effect in a nuclear membrane under the excess gas pressure load and the initial pore radius, pressure loading, pore density and working surface of a sample.

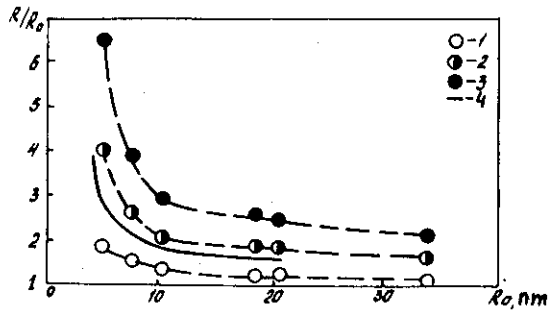

Fig. 5. Experimental relation $R/R_o=f(R_o)$ for the samples with $n = (3\div4)10^8$ cm^{-2} and $S=0.196$ cm^2. 1,2,3, $P_l=0.4$; 0.6; 0.75 MPa; 4, P_l = 0.4 MPa and $n=10^7$ cm^{-2}.

4. Viscoelastic properties of polymeric membranes

As is known, polymeric materials are deformed in a viscoelastic manner. In particular, their viscoelastic properties are determined by the dependence of the relative deformation of samples on the time of action of the constant tension /11/. In experiments on the loading of the nuclear membranes the relaxation character of the deformation can be observed by the dependence of the gas flow rate through the membrane on the loading and off-loading time, i.e. in loading and off-loading cycles. The table lists the data of the gas flow rate Q^* vs. the time for the sample with the $R_o=(7.5\pm0.4)$ nm, $n=(3.6\pm0.5)\times 10^8$ cm^{-2} and $S=(0.95\pm0.03)$ cm^2 obtained in a loading and off-loading cycle. The loading was carried out by the "shock" method. Argon was used as the working gas. The time of the loading was about 20 minutes.

If one writes down the equation for the volume gas flow rate in the Knudsen flow regime as

$$Q=\frac{2}{3}\cdot\frac{\pi R^3}{l}V_t\cdot\frac{\Delta P}{P_o}N\frac{2-\varepsilon}{\varepsilon}, \qquad (3)$$

(here V_t is the mean thermal velocity of gas molecules; ε is the accomodation coefficient of the tangential momentum on the pore walls, for argon it is found to be 0.99 /8/; l is the membrane thickness; N is the total number of pores), then the cube root of the

Table

Experimental relation $Q^* = f(t)$ in loading and off-loading cycle

P_l, MPa	Loading			Off-loading		
	t, min	$Q^* \cdot 10^2$, cm^3/s	R/R_o	t, min	$Q^* \cdot 10^2$, cm^3/s	R/R_o
0.04	1.5	1.22		3	1.2	
	9.5	1.30				
	20	1.31				
0.08	1.5	1.48		3	1.24	
	11	1.57		15	1.21	
	20	1.61				
0.1	2	1.7	1.12	2	1.41	
	12	1.8	1.165	13	1.35	
	20	1.94	1.175	47	1.33	
0.2	1	14	2.27	7	7.36	1.83
	5.5	15.8	2.37	17	6.48	1.75
	12	16.5	2.40	40	5.81	1.69
	19	16.9	2.41	56	5.65	1.67
0.35	1	93.7	4.14	5	52.5	3.52
	5	103	4.28	17	50.6	
	10	108	4.34	38	48.6	3.43
	19	112	4.39	62	47.6	
	185	114	4.42	102	46.9	3.39

ratio Q^*/Q^*_o (Q^*_o is the gas flow rate through the unloaded sample) will yield the information about the ratio of the pore radii before and after loading. So, Fig.6 represents the corresponding dependences for the fourth and fifth loading and off-loading cycles. The behavior of the curves shows that at the moment of the load application the pore deformation process (growth) begins in a polymeric nuclear membrane. The process develops in time and is characterized by the elastic, elastic time-lag and irreversible deformation of the plastic flow in the around-pore areas. The end of the development of the elastic time-lag deformation of the polymer may be related to the tending of the curves to a conditional plateau. The time of the tending is about 0.3-0.5 h and is determined by both the geometric and strength features of the samples.

When the load is removed, the elastic deformation first vanishes, and then the decrease in the pore size continues on account of

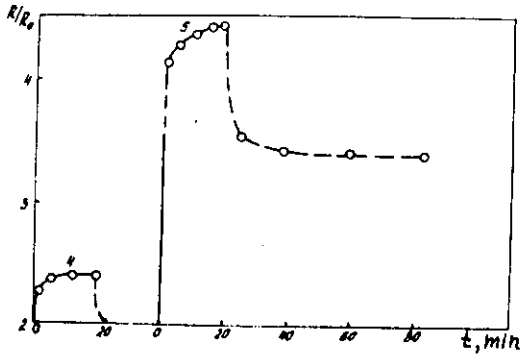

Fig. 6. Experimental relation $R/R_o=f(t)$ for the sample with $R_o=7.5$ nm, $n=3\ 10^8$ cm^{-2} and $S=0.95$ cm^2 in the fourth and fifth cycles of the loading and off-loading.

the elastic time-lag deformation of the polymer. Similarly to what was said above the visible relaxation processes in the membranes finish 0.3-1.5 h after the load is removed. At last the final pore size, exceeding the initial one, can be related only to the irreversible plastic deformation of polymer in the around-pore areas of the membrane. The described relaxation process was observed in the experiments with the nuclear membranes with the pore size larger than 20 nm. The relaxation behavior typical of the membranes with fine-sized channels is complicated by the surface tense effects (Laplace pressure) and is not discussed here.

Thus, on the basis of the viscoelastic representation of the deformation of the polymeric nuclear membrane it is shown that the controllable pore growth in a membrane under load is related only to the plastic deformation in the around-pore areas. This is characteristic of the membrane with the stable final size of channels in absence of the forces leading to pore shrinkage /7/.

5. Conclusion

The loading of the polymeric nuclear membranes by a pressure difference (i.e. the loading pressure exceeds some threshold value) leads to a considerable pore growth reaching hundreds per cent. The dependence of the pore growth on the pressure load, initial pore radius, pore density and working surface of the sample experimentally determined.

The most stable behavior of the deformed membranes is observed for the pore size larger than 20 nm, which is due to the absence of the "healing" effects caused by the surface tension force (Laplace pressure). The behaviour of the membrane under pressure load was explained on the basis of the viscoelastic deformation consisting of the elastic, elastic time-lag and plastic components. The experimental investigation of a membrane in loading and off-loading cycles confirmed that the irreversible increase in the permeability is caused by the plastic deformation appearing in the around-pore zones. The relaxation processes in a PETP nuclear membrane at room temperature can last for 0.3-1.5 h.

Finally, the authors would like to thank O.L.Orelovich for the experiments with scanning electron microscope JSM-840 that confirmed our data, and Professor B.T.Porodnov for fruitful discussions.

References

1. E.P.Ageev, A.N.Neverov, N.L.Strusovskaya et al. Vestn. Mosc. Univ. (USSR). 23 (1982) 75.
2. M.A.Krykin, V.V.Lomakin, O.I.Tigina et al. J. Chem. Phys. (USSR). 60 (1986) 878.
3. A.G.Aleskerov, A.L.Volynskii, N.F.Bakeev. Vysokomol. Soed. (USSR) A18 (1976) 2121.
4. A.L.Volynskii, V.S.Loginov et al. Vysokomol. Soed. (USSR). A22 (1980) 2727.
5. A.L.Volynskii, O.V.Kozlova, V.V.Lavrent'ev. Vysokomol. Soed. (USSR) A27 (1985) 2169.
6. G.N.Flerov. Vestnik Acad. Nauk (USSR) 4 (1984) 35.
7. V.V.Ovchinnikov, V.D.Seleznev, V.I.Kuznetsov et al. Report of JINR,P18-87-637 (Dubna, 1987).
8. V.V.Surguchev, V.D.Seleznev, V.V.Ovchinnikov et al. Preprint of JINR, 18-87-624 (Dubna, 1987).
9. V.I.Kuznetsov, V.V.Ovchinnikov, V.D.Seleznev et al. Eng. Phys. J. (USSR). 45 (1983) 332.
10. S.F.Borisov, B.A.Kalinin, et al. Pribory i Tech. Exp. (USSR). 4 (1972) 209.
11. A.A.Tager. Fisico-Chimiya Polimerov. Moscow, Chimiya, 1968.

Received by Publishing Department
on March 13, 1989.